Environmental Science & Technology Letters

pubs.acs.org/journal/estlcu

Letter

Facile Synthesis of Electrically Conductive Membranes

Wei Zhang, Nick Guan Pin Chew, and Orlando Coronell*

Cite This: https://doi.org/10.1021/acs.estlett.3c00631

Read Online

ACCESS | Metrics & More | Article Recommendations | Supporting Information

ABSTRACT: A facile and effective strategy that can be used to fabricate electrically conductive membranes (ECMs) of diverse filtration performance (i.e., water productivity and solute rejection) is not available yet. Herein, we report a facile method that enables the fabrication of ECMs of a broad performance range. The method is based on the use of polyethylenimine (PEI), glutaraldehyde, and any of a diverse set of conductive materials to cast an electrically conductive layer atop any of a diverse set of substrates (i.e., from microfiltration to reverse osmosis membranes). We developed the reported ECM fabrication method using graphite as the conductive material and PVDF membranes as substrates. We demonstrate that graphite-PVDF ECMs were stable and electrically conductive and could be successfully used for solute filtration and electrochemical degradation. We also confirmed that the PEI/glutaraldehyde-based ECM fabrication method is suitable for conductive materials other than graphite, including carbon nanotubes, reduced graphene oxide, activated charcoal, and silver nanoparticles. Compared with the substrates used for their fabrication, ECMs showed low electrical sheet resistances that varied with conductive material, increased solute rejection, and reduced water permeance. Taken together, this work presents a promising general strategy for the fabrication of ECMs for environmental applications from diverse substrates and conductive materials.

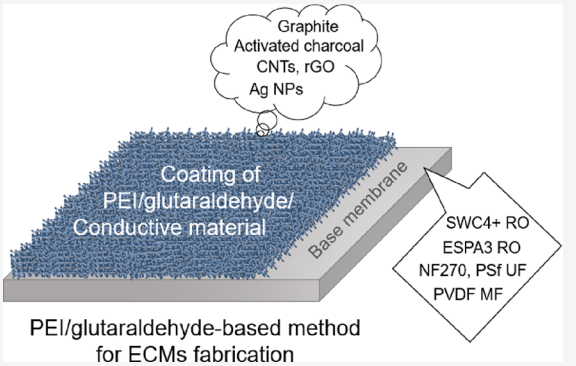

KEYWORDS: *conductive materials, polyethylenimine, graphite, carbon nanotubes, activated charcoal, silver nanoparticles, electrically conductive membranes*

INTRODUCTION

Water is essential for life on Earth, as well as global economic development. However, water scarcity has been accelerating due to rapid industrialization, population growth, and climate change.[1,2] To address the water crisis, membrane-based seawater/brackish-water treatment and wastewater reclamation have been widely utilized for producing potable and irrigation water.[3−5] In spite of the commercial success of membrane separation technologies, improvements in membranes and membrane processes are still needed to address existing challenges such as membrane fouling and low (or no) removal/degradation of some targeted contaminants.[6−8] One such innovation is the utilization of electrically conductive membranes (ECMs) due to their self-cleaning efficiency and simultaneous oxidation/reduction ability over long-term operation.[9−12] By applying an electric potential to an ECM, the membrane exerts strong electrostatic repulsion against contaminants.[13,14] Under applied voltages, the membrane can also generate strong oxidizing species (e.g., reactive oxygen and chlorine species) that could inactivate attached microorganisms,[15] reduce/oxidize toxic heavy metal ions (e.g., arsenite-(III) and chromium(VI)),[12,16] and degrade contaminants on membrane surfaces/pores or in water.[17]

To fabricate ECMs, the choice of conductive material is a critical consideration.[18] Since most conductive metal particles/nanoparticles (e.g., silver (Ag) and copper) are relatively costly and tend to leach into solution,[19] carbon-based materials including graphene,[20] reduced graphene oxide (rGO),[19] and carbon nanotubes (CNTs)[14,21] have been evaluated in recent years, with the latter being the most widely reported. In terms of the method used to render membranes electrically conductive, poly(vinyl alcohol) (PVA)-based cross-linking with CNTs or graphene as conductive materials is the most commonly used method for functionalization of ultrafiltration (UF) membranes,[12,22−24] whereas the only reported approach for functionalization of polyamide-based osmotic membranes is the physical blending of polymer and CNTs or other conductive materials (e.g., carbon particles) during polyamide layer formation.[25,26] Although ECMs fabricated via the aforementioned approaches show excellent potential in water/wastewater treatment applications, a simple and cost-effective fabrication method that could be used to realize ECMs of diverse filtration performance using diverse substrates

Received: September 4, 2023
Revised: September 26, 2023
Accepted: September 27, 2023

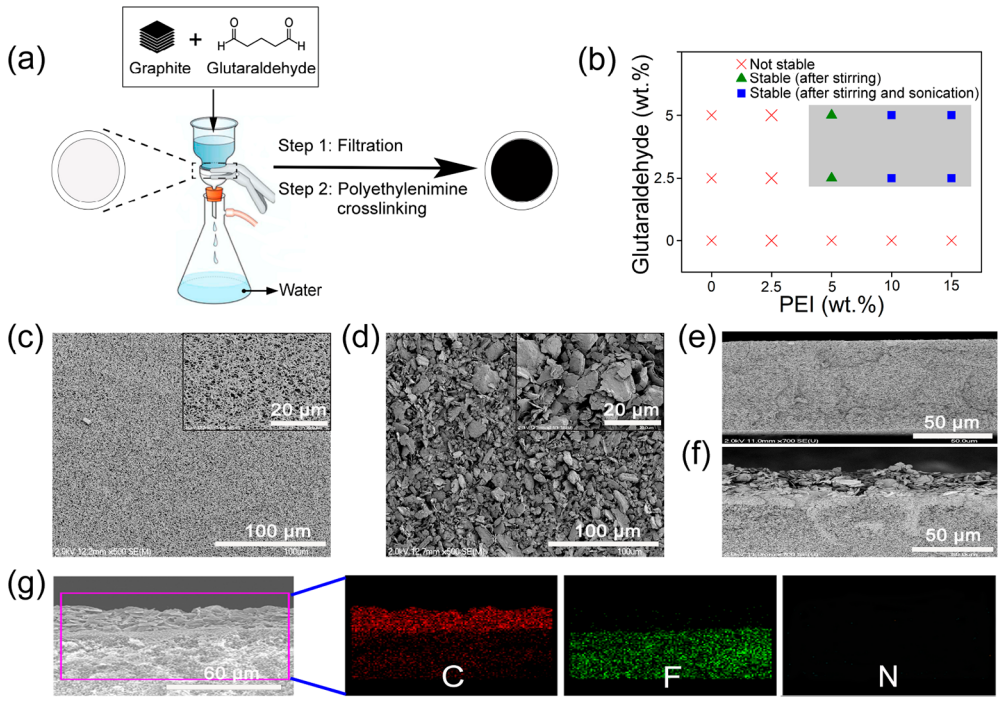

Figure 1. Schematic diagrams of (a) the filtration setup used to prepare graphite-PVDF ECMs (see more details in Figure S4) and (b) physical stability of membranes after overnight stirring (130 rpm) followed by sonication (5 h, 50 °C) in LGW. The *x*-axis and *y*-axis values in (b) indicate the range of membrane fabrication conditions studied; the ECM fabricated with graphite, 2.5 wt % glutaraldehyde, 10 wt % PEI, and the PVDF 0.1 μm substrate is termed the g/PVDF-m1 ECM. Representative (c, d) SEM top-view, (e, f) SEM cross-section, and (g) EDS cross-section elemental mapping of the (c, e) unmodified PVDF 0.1 μm substrate and (d, f, g) g/PVDF-m1 ECM. g/PVDF-m1 ECM fabrication conditions: 8 mL of 20 mg/mL graphite in aqueous solution with 2.5 wt % glutaraldehyde was filtered through a 96 mm diameter coupon of a PVDF 0.1 μm substrate via vacuum filtration, and then, 0.4 mL of 10 wt % PEI in ethanol was poured on membrane.

(e.g., reverse osmosis (RO), nanofiltration (NF), ultrafiltration (UF), and microfiltration (MF) membranes) and conductive materials would significantly contribute to facilitating broader ECM implementation.

In this study, we report a facile and cost-effective method for the fabrication of ECMs using different types of conductive materials and nonconductive substrates. The method uses polyethylenimine (PEI), glutaraldehyde, and a conductive material (e.g., inexpensive graphite) to modify a nonconductive substrate. We first optimized the ECM fabrication method using ECM stability as the criterion, graphite as the conductive material, and PVDF membranes as substrates. Then, we demonstrated that the proposed fabrication method can be used with a broad range of commercial substrates (i.e., MF, UF, NF, and RO) and conductive materials (i.e., CNTs, rGO, activated charcoal, and Ag nanoparticles (NPs)). We also demonstrated the stability of ECMs under various water and stress conditions and ability of ECMs to filter solutes out of water and degrade a model organic contaminant (i.e., methylene blue (MB)) as an illustrative application of ECMs.

METHODS AND MATERIALS

Synthesis of Electrically Conductive Membranes. Substrates (i.e., commercial membranes) were washed with 50 vol % ethanol for 24 h at room temperature to remove impurities from the surface and pores. For ECM fabrication using graphite as the conductive material, a graphite solution (20 mg/mL in laboratory-grade water (LGW)) containing glutaraldehyde (0−5 wt %) was prepared and stirred at 130 rpm overnight. Next, 2−12 mL of the graphite-glutaraldehyde solution was filtered through the substrate (active area of 12.56 cm^2) by either vacuum filtration (i.e., 0.1−0.8 μm PVDF membranes) or dead-end filtration at 200 psi (i.e., PSf 20 kDa, NF270, ESPA3, and SWC4+ membranes). Then, 0.1−0.6 mL of a PEI solution (0−15 wt % in ethanol) was gently added to the graphite-covered substrate surface for glutaraldehyde-PEI cross-linking and air-dried for a few minutes. The volume ratio between glutaraldehyde and PEI solutions was always 20:1. The resulting ECM was immersed in LGW and stirred at 130 rpm for 12 h to remove any loosely attached graphite particles and noncross-linked PEI. The resulting membrane was stored in LGW at room temperature until use. ECMs were also fabricated using the same procedure but with CNTs, rGO, activated charcoal, or Ag NPs as the conductive material.

Characterization of Membranes. Physical and chemical properties of substrates and ECMs were evaluated by common membrane characterization procedures such as microscopy and spectroscopy methods (Section S1). The physical stability of ECMs was assessed via visual inspection (i.e., absence of conductive layer detachment indicated stability; Section S1) and/or evaluation of change in sheet resistance (i.e., <5% change in sheet resistance indicated stability; Section S1). ECM water permeance and salt rejection were evaluated via dead-end filtration without applied voltage. MB degradation by ECMs was evaluated using a batch electrochemical reaction setup (i.e., ECM as cathode, platinum (Pt) as anode), and simultaneous MB rejection and degradation were evaluated via dead-end filtration with and without applied voltage (Section S1). The MB concentration in solution was obtained from the solution absorbance at 664 nm (HP 8452A, USA). The total oxidant concentration in solution was measured using the N,N-diethyl-p-phenylenediamine (DPD) colorimetric method.[27−29]

https://doi.org/10.1021/acs.estlett.3c00631
Environ. Sci. Technol. Lett. XXXX, XXX, XXX−XXX

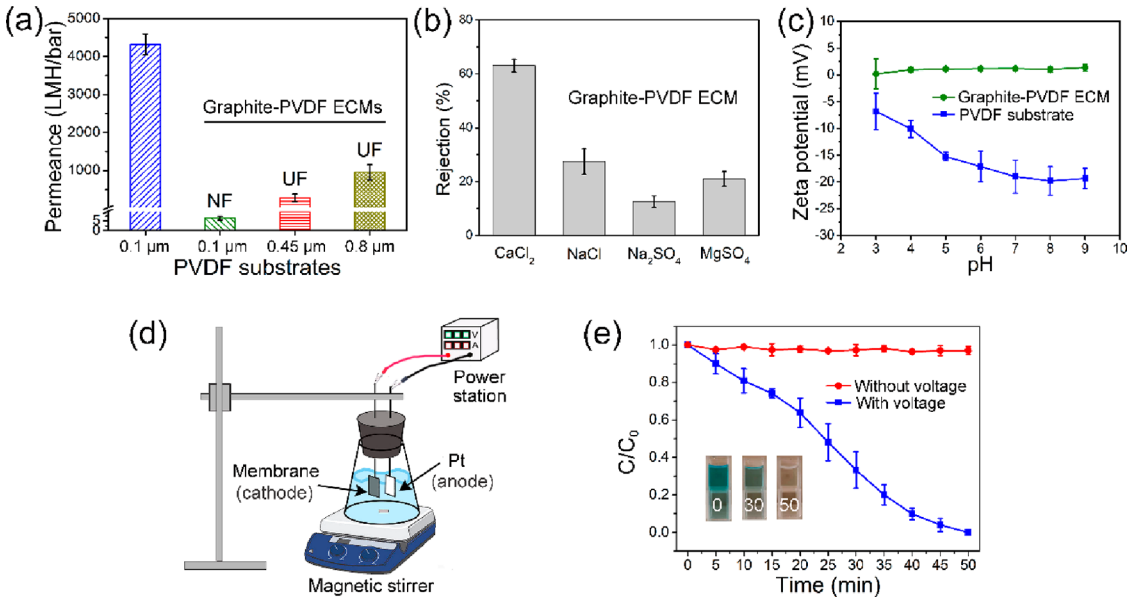

Figure 2. (a) Water permeance and (b) single-salt rejection of a graphite-PVDF ECM (g/PVDF-m1) when filtering 1 g/L feed salt solutions. (c) Zeta potential of pristine PVDF 0.1 μm substrate and the graphite-PVDF ECM (g/PVDF-m1) in 1 mM KCl under different solution pH conditions. (d) Schematic illustration of a batch electrochemical oxidation system used for MB degradation (100 mL, 30 mg/L MB, 100 mM NaCl). (e) Batch MB degradation with time with (5 V) and without applied voltage using a graphite-PVDF ECM (g/PVDF-m1) and the system in panel d. Error bars represent the standard deviation ($n \geq 3$). ECM fabrication conditions: 8 mL of 20 mg/mL graphite in aqueous solution with 2.5 wt % glutaraldehyde was filtered through a 96 mm diameter coupon of a PVDF substrate via vacuum filtration, and then, 0.4 mL of 10 wt % PEI in ethanol was poured on membrane.

RESULTS AND DISCUSSION

Fabrication of Graphite-Based ECMs. Figure 1a and Figure S4 illustrate the synthesis of electrically conductive membranes (ECMs) using the proposed PEI/glutaraldehyde-based fabrication method, graphite as the conductive material, and PVDF as the substrate. Results show that graphite-PVDF ECMs were not stable when using PEI only, glutaraldehyde only, or both with a PEI concentration <5 wt % (Figure 1b, Table S1). Although graphite-PVDF ECMs obtained with a PEI concentration of 5 wt % together with a glutaraldehyde concentration ≥2.5 wt % were stable after overnight stirring, those membranes were not stable under sonication (Figure 1b, Figure S5, Table S1). By contrast, when ≥10 wt % PEI together with ≥2.5 wt % glutaraldehyde was used, the resulting graphite-PVDF ECMs were stable after both overnight stirring and sonication in the pH range of 3−11, batch MB degradation tests, and MB filtration tests with and without an applied voltage (1 h) (Figure 1b, Figures S5 and S6, Table S1). Evaluation of ECM stability under long-term operation is needed in future studies for ECMs intended to be upscaled for, e.g., pilot studies. Considering that a greater PEI concentration might result in lower water permeance because of potential greater cross-linking of the conductive layer, 2.5 wt % glutaraldehyde and 10 wt % PEI were selected as the optimized condition for preparation of graphite-based ECMs for subsequent tests.

The changes in the membrane surface and cross-section microstructure resulting from graphite layer casting were evaluated by scanning electron microscopy (SEM). The original PVDF substrate showed a relatively smooth surface with a homogeneous distribution of surface pores (Figure 1c), whereas graphite particles were present across all the graphite-PVDF ECM surfaces (Figure 1d). The graphite-PVDF ECM had a surface roughness measured by AFM on the ∼1 μm scale, which is about 4−5 times greater than that of the original PVDF substrate (Figure S7). The graphite layer in the ECM was also evident in the cross-sectional SEM images with a thickness of ∼30 μm (Figures 1e−g). The main reason for the relatively large thickness of the conductive layer is the average size of the commercial graphite used (i.e., few to 20 μm, Figure S3); however, within the constraints imposed by the size of the conductive particles, we controlled the thickness of the conductive layer by adjusting the amount of graphite deposited on the substrate (Figure S8). Cross-section energy dispersive spectroscopy (EDS) elemental mapping results (Figure 1g) show that a carbon layer (carbon, C signal) was present on top of the PVDF substrate (fluorine, F signal), confirming the successful coating of the substrate with graphite, while a nitrogen (N) signal from PEI was not observable in the graphite layer of the graphite-PVDF ECM due to low sensitivity of EDS for nitrogen.[30,31] X-ray photoelectron spectroscopy (XPS), Raman spectroscopy, and attenuated total reflection Fourier-transform infrared (FTIR) spectroscopy results also confirmed the casting of the graphite layer and cross-linking between glutaraldehyde and PEI (Section S2). Thanks to the successful coating of the substrate with a stable cross-linked graphite layer, the graphite-PVDF ECM is electrically conductive. The synthesized graphite-PVDF ECM showed a sheet resistance (3.2 ± 1.5 kΩ/sq) lower than most of those reported for conductive membranes/thin films in the literature (Table S2).

Filtration Performance and MB Degradation by Graphite-Based ECMs. We evaluated the water permeance and salt rejection of PVDF substrates and PVDF-graphite ECMs (Figure 2a, b). Results (Figure 2a) show that the water permeance of the graphite-PVDF ECM was substantially lower (7 L/m^2/h/bar) than that of the original PVDF substrate (∼4300 L/m^2/h/bar) due to added resistance to water

https://doi.org/10.1021/acs.estlett.3c00631
Environ. Sci. Technol. Lett. XXXX, XXX, XXX−XXX

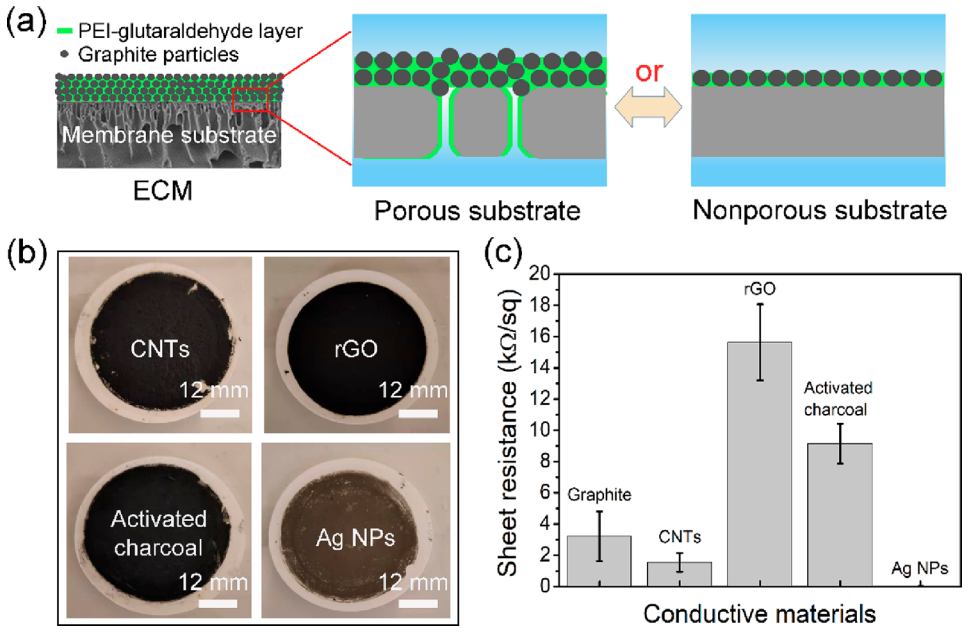

Figure 3. (a) Schematic of proposed physical interlocking between the conductive layer and the substrate in ECMs synthesized using the PEI/glutaraldehyde-based fabrication method. (b) Images of ECMs prepared using a PSf 20 kDa membrane as substrate, diverse conductive materials (i.e., CNTs, rGO, activated charcoal, Ag NPs) and the proposed PEI/glutaraldehyde-based fabrication method. (c) Sheet resistance of membranes in (b) after stirring in water overnight. ECM fabrication conditions: 4 mL of 20 mg/mL active material with 2.5 wt % glutaraldehyde was filtered through a 48 mm diameter coupon of a PSf 20 kDa membrane at 200 psi, and then, 0.2 mL of 10 wt % PEI in ethanol was poured on the membrane. Error bars represent standard deviation ($n \geq 5$).

transport by the conductive layer. Although the graphite-PVDF ECM had a low water permeance, the ECM permeance can be tailored by using different substrates and thicknesses of the conductive layer. Specifically, we showed that a bigger pore size substrate (e.g., 0.45 and 0.8 μm) resulted in ECMs with higher water permeance in the NF to UF performance range (Figure 2a). Additionally, coating the substrate with a smaller amount of graphite led to thinner conductive layers and higher permeance (Figure S8). Salt rejection results (Figure 2b) show that the graphite-PVDF ECM rejected different salts in decreasing order: $CaCl_2$ > NaCl > $MgSO_4$ > Na_2SO_4. This order is consistent with the rejection order of positively charged NF membranes[32,33] and the slight positive charge of the graphite-PVDF ECM (Figure 2c). The nanofiltration behavior of the graphite-PVDF ECM was supported by its low molecular weight cutoff (~2 kDa; Figure S9). The lower water permeance and higher solute rejection of ECMs compared with the original substrates indicate that the two would likely not be used in the same filtration applications. Further development of the fabrication method is needed to optimize filtration performance (e.g., increase water permeability).

To demonstrate the possible applications of graphite-PVDF ECMs, dye degradation was demonstrated via batch MB electrochemical degradation under an applied voltage (5 V; Figure 2d). The graphite-PVDF ECM served as the cathode and a platinum electrode as the anode. Results show that MB completely degraded over 1 h (Figure 2e) while the ECM remained stable (Table S1). This demonstrates that the graphite-PVDF ECM is stable under applied voltage and can be potentially used in water/wastewater treatment applications for, e.g., electrochemical degradation of contaminants. The solution pH was stable during this experiment, which is consistent with results by Halali et al.[14] The reason why the pH does not change is the simultaneous production of protons at the anode ($2H_2O \rightarrow O_2 + 4H^+ + 4e^-$) and hydroxyl ions at the cathode ($2H_2O + 2e^- \rightarrow 2OH^- + H_2$) that neutralize each other in the bulk solution.

In addition to their evaluation for batch MB electrochemical degradation, graphite-PVDF ECM was evaluated for MB dead-end filtration with and without an applied voltage (30 mg/L MB in 100 mM NaCl solution). Results showed that in the absence of an applied voltage MB concentration increased with time in both the feed and permeate, consistent with the decreasing feedwater volume and relatively high MB rejection (~90%) by the ECM (Figure S10a). By contrast, under applied voltage, the MB concentration decreased with time in both the feed and permeate waters (Figure S10a). Similar to work by others,[29,34] we attribute MB degradation under an applied voltage (Figure 2e and Figure S10a, c) to conversion of MB to CO_2 and H_2O by continuously generated oxidants (e.g., chlorine and hydrogen peroxide) at the anode (Pt) and cathode (ECM). Measurements of total oxidant concentration in solution (i.e., Cl_2, H_2O_2) in control batch tests with ECMs confirmed that oxidants were produced and accumulated under the applied voltage (Figure S10d).

The filtration results also show that the ECM flux decline rate (i.e., fouling) under an applied voltage was 42% lower than that without a voltage (Figure S10b). Given that the ECM was used as the cathode (i.e., negatively charged), MB is positively charged in solution, and MB was the only foulant in solution, the results indicate that the lower flux decline under an applied voltage was the result of MB degradation on the ECM surface and/or inside its pore (i.e., self-cleaning performance).

Applicability of Proposed Fabrication Method to Different Substrates. We evaluated the general applicability of the proposed PEI/glutaraldehyde-based method for ECM fabrication by using four other commercial substrates (i.e., PSf 20 kDa, NF270, ESPA3, and SWC4+ membranes) with

https://doi.org/10.1021/acs.estlett.3c00631
Environ. Sci. Technol. Lett. XXXX, XXX, XXX−XXX

graphite as the active material. Using 2.5 wt % glutaraldehyde and 10 wt % PEI, physically stable ECMs were synthesized using two different amounts of graphite (photos in Figure S11a, b). Results demonstrated the general applicability of the proposed PEI/glutaraldehyde-based fabrication procedure to diverse substrates.

As mentioned above for the PVDF 0.1 μm membrane, the thickness of the graphite layer on porous substrates can be tailored up to at least several tens of micrometers by controlling the amount of graphite deposited on the substrate (i.e., at least ~45 μm, ~32 μm, and ~37 μm for PVDF 0.1 μm, PSF 20 kDa, and NF270 substrates, respectively; Figures S8 and S12a, b). By contrast, the graphite layer was unstable above a thickness of ~20 μm for the nonporous substrates (i.e., ESPA3 and SWC4+; Figures S11 and S12c, d). A plausible explanation for the graphite layer instability on nonporous substrates for graphite layer thicknesses over ~20 μm is as follows. For porous substrates, the graphite layer is stabilized by polymer cross-linking both on the substrate surface and inside substrate pores; however, for nonporous substrates only surface cross-linking occurs therefore resulting in reduced physical interlocking between the graphite layer and the substrate (Figure 3a). This interpretation is supported by the significantly greater flux decline observed for the porous substrates (98% for PVDF 0.1 μm and 90% for PSf 20 kDa) compared with the nonporous substrates (80% for ESPA3 and 65% for SWC4+) under the same ECM fabrication conditions (Figure S13). When using the same conductive layer casting conditions, we did not observe major differences in stability between porous substrates or between nonporous substrates, and therefore, we do not know if surface roughness (understood beyond differences accounted for by pores) affects conductive layer stability. Further studies are needed to evaluate the specific role of roughness on stability across. Despite the lesser thickness of stable graphite layers on nonporous substrates (15−20 μm) compared with porous substrates (30−40 μm) (Figure S12), all ECMs prepared with graphite had similar sheet resistance (i.e., <3.2 and <2.8 kΩ/sq for ECMs prepared with nonporous and porous substrates, respectively; Table S2). Therefore, we did not observe a strong correlation between the electrical resistance and conductive layer thickness.

Applicability of Proposed Fabrication Method to Different Conductive Materials. In addition to graphite, other conductive materials, including CNTs, rGO, activated charcoal, and Ag NPs (Figure S14a−d), were used to fabricate ECMs using PSf 20 kDa substrates. The images of synthesized ECMs (Figure 3b) and their XRD patterns (Figure S14e) confirm that the proposed glutaraldehyde/PEI-based method was successful, regardless of the conductive material. While for the specific fabrication conditions used (i.e., 2.5 wt % glutaraldehyde, 10 wt % PEI, filtration-based deposition of conductive particle on substrate) conductive material identity did not impact ECM stability, we did not evaluate a broader range of fabrication conditions with diverse conductive particles. Therefore, further studies are needed to understand the effect of particle properties on ECM stability. Membrane sheet resistance results (Figure 3c, Table S2) indicate that ECM electrical conductivity varied with the conductive material. Graphite stood out because despite being the cheapest material it resulted in competitive resistances (3.2 ± 1.5 kΩ/sq); CNTs resulted in ECMs with half the resistance (1.5 ± 0.6 kΩ/sq) of those prepared with graphite. Ag NPs yielded ECMs with the lowest resistance (<0.02 kΩ/sq).

Permeation results (Figure S15) show that ECMs synthesized with PSf 20 kDa substrates and diverse conductive materials displayed water permeances in the RO (~1 to few L/m^2/h/bar) to NF (few to <20 L/m^2/h/bar) range[35] and NaCl rejection in the NF range (i.e., few to tens of percentage points), when challenged with a 1 g/L NaCl solution. Ag NPs were the conductive material that resulted in the lowest water permeance (~7.7 L/m^2/h/bar) and the highest NaCl rejection (~32%). The results therefore indicate that it is viable to produce ECMs with NF filtration performance and potentially RO filtration performance using our ECM fabrication method. Further work is needed to optimize filtration performance.

Overall, we demonstrated a facile ECM fabrication method that uses relatively low-cost and common materials (e.g., PEI, glutaraldehyde, and ethanol) and is suitable for ECM fabrication from diverse commercial substrates and conductive materials. One drawback of this method is that the filtration-based procedure used for depositing the conductive particles on the substrates is not easily scalable. Therefore, there is a need to evaluate alternate approaches for conductive particle deposition that are more translationally relevant (e.g., spray-based techniques used in RO membrane fabrication[36−38]). Using the current bench-scale fabrication method, the estimated cost of the fabrication materials different from the substrate is approximately \$4/m^2 (Table S3). Given that the method has not been optimized nor adapted for scalability, and that the retail cost of a seawater desalination membrane is approximately \$20/m^2,[39] the proposed ECM fabrication method appears economically promising for upscaling. Technical improvements for scalability (e.g., spray-based deposition of conductive particles on a substrate) and optimization of material utilization (e.g., decreasing the conductive layer thickness) will contribute to improving the economics of the method. The reported ECM fabrication method could find applications in water and wastewater treatment, where simultaneous separations and oxidation/reduction would be advantageous.

■ ASSOCIATED CONTENT

Supporting Information

The Supporting Information is available free of charge at https://pubs.acs.org/doi/10.1021/acs.estlett.3c00631.

Additional materials, methods, and supporting materials and membrane characterization results (PDF)

■ AUTHOR INFORMATION

Corresponding Author

Orlando Coronell − *Department of Environmental Sciences and Engineering, Gillings School of Global Public Health, University of North Carolina at Chapel Hill, Chapel Hill, North Carolina 27599, United States;* orcid.org/0000-0002-7018-391X; Email: coronell@unc.edu

Authors

Wei Zhang − *Department of Environmental Sciences and Engineering, Gillings School of Global Public Health, University of North Carolina at Chapel Hill, Chapel Hill, North Carolina 27599, United States;* orcid.org/0000-0002-1912-8077

https://doi.org/10.1021/acs.estlett.3c00631
Environ. Sci. Technol. Lett. XXXX, XXX, XXX−XXX

Nick Guan Pin Chew − *Department of Environmental Sciences and Engineering, Gillings School of Global Public Health, University of North Carolina at Chapel Hill, Chapel Hill, North Carolina 27599, United States;* orcid.org/0000-0001-7634-537X

Complete contact information is available at: https://pubs.acs.org/10.1021/acs.estlett.3c00631

Notes

The authors declare the following competing financial interest(s): A provisional patent application (PCT/US2023/022273) has been filed by the University of North Carolina at Chapel Hill on technology related to electrically conductive membranes.

■ ACKNOWLEDGMENTS

This research was partially funded by a grant from the National Institute of Environmental Health Sciences (P42ES031007). The authors would like to thank Dr. Amar S. Kumbhar from Chapel Hill Analytical and Nanofabrication Laboratory (CHANL) for his assistance in the acquisition of SEM and AFM images and Dr. Carrie Donley for her assistance with XPS analysis. A portion of this work was performed using the Raman spectroscopy instrumentation in the CHASE Hub Instrumentation Facility established by the Center for Hybrid Approaches in Solar Energy to Liquid Fuels (CHASE), an Energy Innovation Hub funded by the U.S. Department of Energy, Office of Science, Office of Basic Energy Sciences under Award Number DE-SC0021173.

■ REFERENCES

(1) Zhang, R.; Liu, Y.; He, M.; Su, Y.; Zhao, X.; Elimelech, M.; Jiang, Z. Antifouling Membranes for Sustainable Water Purification: Strategies and Mechanisms. *Chem. Soc. Rev.* **2016**, *45* (21), 5888−5924.

(2) Shannon, M. A.; Bohn, P. W.; Elimelech, M.; Georgiadis, J. G.; Mariñas, B. J.; Mayes, A. M. Science and Technology for Water Purification in the Coming Decades. *Nature* **2008**, *452* (7185), 301−310.

(3) Subramani, A.; Jacangelo, J. G. Emerging Desalination Technologies for Water Treatment: A Critical Review. *Water Res.* **2015**, *75*, 164−187.

(4) Obotey Ezugbe, E.; Rathilal, S. Membrane Technologies in Wastewater Treatment: A Review. *Membranes* **2020**, *10* (5), 89.

(5) Elimelech, M.; Phillip, W. A. The Future of Seawater Desalination: Energy, Technology, and the Environment. *Science* **2011**, *333* (6043), 712−717.

(6) Zhang, W.; Cheng, W.; Ziemann, E.; Be'er, A.; Lu, X.; Elimelech, M.; Bernstein, R. Functionalization of Ultrafiltration Membrane with Polyampholyte Hydrogel and Graphene Oxide to Achieve Dual Antifouling and Antibacterial Properties. *J. Membr. Sci.* **2018**, *565*, 293−302.

(7) Larocque, M. J.; Gelb, A.; Latulippe, D. R.; de Lannoy, C. F. Meta-Analysis of Electrically Conductive Membranes: A Comparative Review of Their Materials, Applications, and Performance. *Sep. Purif. Technol.* **2022**, *287*, 120482.

(8) Cheng, W.; Lu, X.; Kaneda, M.; Zhang, W.; Bernstein, R.; Ma, J.; Elimelech, M. Graphene Oxide-Functionalized Membranes: The Importance of Nanosheet Surface Exposure for Biofouling Resistance. *Environ. Sci. Technol.* **2020**, *54* (1), 517−526.

(9) Ahmed, F.; Lalia, B. S.; Kochkodan, V.; Hilal, N.; Hashaikeh, R. Electrically Conductive Polymeric Membranes for Fouling Prevention and Detection: A Review. *Desalination* **2016**, *391*, 1−15.

(10) Li, R.; Wu, Y.; Shen, L.; Chen, J.; Lin, H. A Novel Strategy to Develop Antifouling and Antibacterial Conductive Cu/Polydopamine/Polyvinylidene Fluoride Membranes for Water Treatment. *J. Colloid Interface Sci.* **2018**, *531*, 493−501.

(11) Yu, W.; Liu, Y.; Xu, Y.; Li, R.; Chen, J.; Liao, B. Q.; Shen, L.; Lin, H. A Conductive PVDF-Ni Membrane with Superior Rejection, Permeance and Antifouling Ability via Electric Assisted in-Situ Aeration for Dye Separation. *J. Membr. Sci.* **2019**, *581*, 401−412.

(12) Ma, S.; Yang, F.; Chen, X.; Khor, C. M.; Jung, B.; Iddya, A.; Sant, G.; Jassby, D. Removal of As (III) by Electrically Conducting Ultrafiltration Membranes. *Water Res.* **2021**, *204*, 117592.

(13) Dudchenko, A. V.; Rolf, J.; Russell, K.; Duan, W.; Jassby, D. Organic Fouling Inhibition on Electrically Conducting Carbon Nanotube−Polyvinyl Alcohol Composite Ultrafiltration Membranes. *J. Membr. Sci.* **2014**, *468*, 1−10.

(14) Halali, M. A.; de Lannoy, C.-F. Quantifying the Impact of Electrically Conductive Membrane-Generated Hydrogen Peroxide and Extreme pH on the Viability of *Escherichia coli* Biofilms. *Ind. Eng. Chem. Res.* **2022**, *61* (1), 660−671.

(15) Anis, S. F.; Lalia, B. S.; Khair, M.; Hashaikeh, R.; Hilal, N. Electro-Ceramic Self-Cleaning Membranes for Biofouling Control and Prevention in Water Treatment. *Chem. Eng. J.* **2021**, *415*, 128395.

(16) Thamaraiselvan, C.; Thakur, A. K.; Gupta, A.; Arnusch, C. J. Electrochemical Removal of Organic and Inorganic Pollutants Using Robust Laser-Induced Graphene Membranes. *ACS Appl. Mater. Interfaces* **2021**, *13* (1), 1452−1462.

(17) Li, J.; Liu, Q.; Liu, Y.; Xie, J. Development of Electro-Active Forward Osmosis Membranes to Remove Phenolic Compounds and Reject Salts. *Environ. Sci. Water Res. Technol.* **2017**, *3* (1), 139−146.

(18) Sun, M.; Wang, X.; Winter, L. R.; Zhao, Y.; Ma, W.; Hedtke, T.; Kim, J.-H.; Elimelech, M. Electrified Membranes for Water Treatment Applications. *Acs Es&T Eng.* **2021**, *1* (4), 725−752.

(19) Straub, A. P.; Bergsman, D. S.; Getachew, B. A.; Leahy, L. M.; Patil, J. J.; Ferralis, N.; Grossman, J. C. Highly Conductive and Permeable Nanocomposite Ultrafiltration Membranes Using Laser-Reduced Graphene Oxide. *Nano Lett.* **2021**, *21* (6), 2429−2435.

(20) Thakur, A. K.; Singh, S. P.; Kleinberg, M. N.; Gupta, A.; Arnusch, C. J. Laser-Induced Graphene−PVA Composites as Robust Electrically Conductive Water Treatment Membranes. *ACS Appl. Mater. Interfaces* **2019**, *11* (11), 10914−10921.

(21) Ho, K. C.; Teow, Y. H.; Mohammad, A. W.; Ang, W. L.; Lee, P. H. Development of Graphene Oxide (GO)/Multi-Walled Carbon Nanotubes (MWCNTs) Nanocomposite Conductive Membranes for Electrically Enhanced Fouling Mitigation. *J. Membr. Sci.* **2018**, *552*, 189−201.

(22) Ronen, A.; Duan, W.; Wheeldon, I.; Walker, S.; Jassby, D. Microbial Attachment Inhibition through Low-Voltage Electrochemical Reactions on Electrically Conducting Membranes. *Environ. Sci. Technol.* **2015**, *49* (21), 12741−12750.

(23) Halali, M. A.; de Lannoy, C. F. Methods for Stability Assessment of Electrically Conductive Membranes. *MethodsX* **2022**, *9*, 101627.

(24) De Lannoy, C. F.; Jassby, D.; Davis, D. D.; Wiesner, M. R. A Highly Electrically Conductive Polymer−Multiwalled Carbon Nanotube Nanocomposite Membrane. *J. Membr. Sci.* **2012**, *415*, 718−724.

(25) de Lannoy, C. F.; Jassby, D.; Gloe, K.; Gordon, A. D.; Wiesner, M. R. Aquatic Biofouling Prevention by Electrically Charged Nanocomposite Polymer Thin Film Membranes. *Environ. Sci. Technol.* **2013**, *47* (6), 2760−2768.

(26) Xu, X.; Zhang, H.; Yu, M.; Wang, Y.; Gao, T.; Yang, F. Conductive Thin Film Nanocomposite Forward Osmosis Membrane (TFN-FO) Blended with Carbon Nanoparticles for Membrane Fouling Control. *Sci. Total Environ.* **2019**, *697*, 134050.

(27) Bader, H.; Sturzenegger, V.; Hoigné, J. Photometric Method for the Determination of Low Concentrations of Hydrogen Peroxide by the Peroxidase Catalyzed Oxidation of N, N-Diethyl-p-Phenylenediamine (DPD). *Water Res.* **1988**, *22* (9), 1109−1115.

(28) Kosaka, K.; Yamada, H.; Matsui, S.; Echigo, S.; Shishida, K. Comparison among the Methods for Hydrogen Peroxide Measurements to Evaluate Advanced Oxidation Processes: Application of a Spectrophotometric Method Using Copper (II) Ion and 2, 9-

Dimethyl-1, 10-Phenanthroline. *Environ. Sci. Technol.* **1998**, *32* (23), 3821−3824.
(29) Thamaraiselvan, C.; Bandyopadhyay, D.; Powell, C. D.; Arnusch, C. J. Electrochemical Degradation of Emerging Pollutants via Laser-Induced Graphene Electrodes. *Chem. Eng. J. Adv.* **2021**, *8*, 100195.
(30) Wolfgong, W. J. Chemical Analysis Techniques for Failure Analysis: Part 1, Common Instrumental Methods. In *Handbook of Materials Failure Analysis with Case Studies from the Aerospace and Automotive Industries*; Elsevier, 2016; pp 279−307. DOI: 10.1016/B978-0-12-800950-5.00014-4.
(31) Zhang, W.; Huang, H.; Bernstein, R. Zwitterionic Hydrogel Modified Reduced Graphene Oxide/ZnO Nanocomposite Blended Membrane with High Antifouling and Antibiofouling Performances. *J. Colloid Interface Sci.* **2022**, *613*, 426−434.
(32) Kaganovich, M.; Zhang, W.; Freger, V.; Bernstein, R. Effect of the Membrane Exclusion Mechanism on Phosphate Scaling during Synthetic Effluent Desalination. *Water Res.* **2019**, *161*, 381−391.
(33) Zheng, J.; Zhang, X.; Li, G.; Fei, G.; Jin, P.; Liu, Y.; Wouters, C.; Meir, G.; Li, Y.; Van der Bruggen, B. Selective Removal of Heavy Metals from Saline Water by Nanofiltration. *Desalination* **2022**, *525*, 115380.
(34) Panizza, M.; Barbucci, A.; Ricotti, R.; Cerisola, G. Electrochemical Degradation of Methylene Blue. *Sep. Purif. Technol.* **2007**, *54* (3), 382−387.
(35) Yang, Z.; Guo, H.; Tang, C. Y. The Upper Bound of Thin-Film Composite (TFC) Polyamide Membranes for Desalination. *J. Membr. Sci.* **2019**, *590*, 117297.
(36) Chowdhury, M. R.; Steffes, J.; Huey, B. D.; McCutcheon, J. R. 3D Printed Polyamide Membranes for Desalination. *Science* **2018**, *361* (6403), 682−686.
(37) Jiang, X.; Chuah, C. Y.; Goh, K.; Wang, R. A Facile Direct Spray-Coating of Pebax® 1657: Towards Large-Scale Thin-Film Composite Membranes for Efficient CO_2/N_2 Separation. *J. Membr. Sci.* **2021**, *638*, 119708.
(38) Ma, X. H.; Yang, Z.; Yao, Z. K.; Guo, H.; Xu, Z. L.; Tang, C. Y. Interfacial Polymerization with Electrosprayed Microdroplets: Toward Controllable and Ultrathin Polyamide Membranes. *Environ. Sci. Technol. Lett.* **2018**, *5* (2), 117−122.
(39) *Hydranautics Seawater RO Membrane SWC5-LD*. Evoqua Water Technologies LLC. https://www.evoqua.com/en/evoqua/parts--consumables/membranes/seawater-membranes/8-seawater-membranes/Hydranautics-seawater-ro-membrane-swc5-ld/?gclid=CjwKCAjwloynBhBbEiwAGY25dD0vU5hNMG3U_qmBokpc28uMdkYDt_hDPj6KkPGaOS9U5P_NT6XDsxoC0AgQAvD_BwE. (accessed 2023−08−26).

https://doi.org/10.1021/acs.estlett.3c00631
Environ. Sci. Technol. Lett. XXXX, XXX, XXX−XXX